Excitation of Guided Waves in Generally Anisotropic Layers Using Finite Sources

J. J. Ditri
Assoc. Mem. ASME.

J. L. Rose
Assoc. Mem. ASME.

Engineering Science and Mechanics Department, Pennsylvania State University, State College, PA 16802

The excitation of guided wave modes in generally anisotropic layers by finite sized strip sources placed on the surfaces of the layer is examined. The general problem of arbitrarily applied harmonic surface tractions is first solved using the normal mode expansion technique in conjunction with the complex reciprocity relation of elastodynamics. This general solution is then specialized to loading situations modelling those commonly used to excite guided waves in layers for use in nondestructive evaluation. The amplitudes of the generated modes are written as the product of an "excitation function" which depends only on the distribution of the applied tractions and an "excitability function" which depends only on the properties of the specific mode(s) being excited and which determines how receptive the modes are to the applied tractions. Expressions are obtained for the −9 dB wave number and phase velocity bandwidths (σ_β and σ_v, respectively) which determine the widths of the wavenumber or phase velocity excitation spectra at the −9 dB generation point. Finally, the problem of transient loading is addressed by superimposing time harmonic solutions via an integration over the dispersion curves of the layer.

Introduction

Guided waves are finding an increased usage among the nondestructive evaluation (NDE) community for both defect detection and material characterization (Spetzler and Datta, 1990; Rokhlin et al., 1990; Karim et al. 1990; Guo and Cawley, 1992; Mal et al., 1992 and Pilarski and Rose, 1992). The unique properties of the individual guided wave modes which exist in the layer offer a host of possibilities for nondestructively probing the material of which the layer is composed. Because of the different field distributions of the different modes, they each interact differently with the material composing the layer, and hence each carries useful information about the constitution and/or state of the layer.

Before one can fully utilize the diverse nature of the different modes, however, it is necessary to understand fully the manner in which the individual guided wave modes can be introduced into the layer by applied surface tractions. The goal of this paper is to determine the amplitude of each of the propagating modes generated in an anisotropic layer due to arbitrarily applied surface tractions, and to relate the amplitudes of the generated modes to the properties of the tractions used to excite them. After the results are obtained for arbitrary loading, specific loading conditions, typical of those used in nondestructive evaluation techniques for generating waveguide modes, are examined in detail.

The problem of the excitation of an arbitrarily anisotropic layer due to arbitrarily applied time-harmonic surface tractions is solved by utilizing the Normal Mode Expansion Technique (Auld and Kino, 1971; Kino, 1987; Auld, 1990b). In this technique, the fields in the loaded layer are expanded in terms of the "normal modes" of the layer (i.e., the mode fields in the free layer) multiplied by unknown complex amplitudes. The goal is then to determine, from the applied tractions, the expansion amplitudes necessary for evaluation of the fields in the loaded waveguide. Such expansion techniques have been successfully used to solve *edge* load problems for plates (Folk and Herczynski, 1986) and solid circular cylinders (Herczynski and Folk, 1989), as well as side excitation problems for hollow circular cylinders (Ditri and Rose, 1992). The key to the success of the technique is the establishment and use of an orthogonality condition between the free waveguide modes, analogous to the orthogonality of the trigonometric functions used in Fourier Series expansions.

Starting with the expansion amplitudes for the harmonic excitation case, the more general problem of arbitrary time-dependence loading can be treated by linear superposition of harmonic solutions. This type of approach leads to solutions (expansion amplitudes) which are identical in *form* for isotropic or generally anisotropic layers. The difference is accounted for when evaluating the quantities appearing in the solutions. Because of this, the true physical nature of the excitation process becomes clear, unobstructed by the peculiarities of a particular material.

Contributed by the Applied Mechanics Division of THE AMERICAN SOCIETY OF MECHANICAL ENGINEERS for publication in the ASME JOURNAL OF APPLIED MECHANICS.

Discussion on this paper should be addressed to the Technical Editor, Professor Lewis T. Wheeler, Department of Mechanical Engineering, University of Houston, Houston, TX 77204-4792, and will be accepted until four months after final publication of the paper itself in the ASME JOURNAL OF APPLIED MECHANICS.

Manuscript received by the ASME Applied Mechanics Division, July 14, 1992; final revision, Dec. 16, 1992. Associate Technical Editor: S. K. Datta.

Normal Modes

The governing equations for wave propagation in flat, linearly elastic, nonpiezoelectric and generally anisotropic layers, for zero body forces, can be written as

$$\frac{\partial T_{ij}}{\partial x_j} = \rho \frac{\partial^2 u_i}{\partial t^2} \tag{1a}$$

$$T_{ij} = C_{ijkl} \frac{\partial u_k}{\partial x_l} \tag{1b}$$

where $\mathbf{T}$ denotes the Cauchy stress tensor, $\mathbf{u}$ denotes the particle displacement vector, $\mathbf{C}$ denotes the stiffness tensor, and ρ denotes the mass density. Summation convention over repeated subscripts is assumed.

Along with the governing equations, Eqs. (1*a–b*), the normal modes of the layer are required to satisfy traction-free boundary conditions

$$t_i \equiv T_{ij} n_j = 0 \tag{2}$$

at both the upper and lower surfaces of the layer. n_i denotes the components of a unit vector normal to the surfaces of the layer. Solutions to the boundary value problem, Eqs. (1) and (2), can be found in the literature for layers of various classes of anisotropy (Solie and Auld, 1972; Nayfeh et al., 1988; Li and Thompson, 1990).

When propagating in an anisotropic layer, the characteristics of the normal modes (i.e., phase and group velocities, field distributions, etc.) are in general very dependent on the orientation between the wave vector of the mode and the natural or crystallographic coordinate system of the media, when such preferred axes exist (see for instance Datta et al., 1988). In all of the derivations to follow, it is assumed that the "z" coordinate is aligned with the wave vector of the generated mode and that the "y" axis is transverse to the layer (i.e., in the thickness direction). For anisotropic layers, this will generally necessitate a coordinate transformation of the elastic stiffness tensor since, in general, the principal axes of the anisotropic medium will not coincide with the chosen coordinate axes. With this choice of coordinate system (and the subsequent transformation of the elastic stiffness tensor), the fields associated with any given mode are uniform in the "x" coordinate direction. This serves to make the problem one of plane strain in the $y - z$ plane (i.e., $\epsilon_{xx} = \epsilon_{xy} = \epsilon_{xz} \equiv 0$ and $\epsilon_{ij} = \epsilon_{ij}(y, z, t)$ where $i, j \in \{y, z\}$).

The fields caused by the waveguide modes can then be written in the general form

$$\xi(y, z, t) = \bar{\xi}(y) e^{j(\omega t - \beta z)} \tag{3}$$

where $\bar{\xi}(y)$ represents the "modal distribution" or "y" variation of the field, ξ. β is the wave number of the mode which, for a given frequency ω, is determined by a generalized Rayleigh-Lamb type of equation whose form depends on the type of anisotropy exhibited by the layer (Li and Thompson, 1990). Just as in the isotropic case, the wave number β can be real, imaginary, or complex for a given real and positive frequency ω.

Problem Statement and Solution

The problem to be addressed is shown in Fig. 1. A linearly elastic, generally anisotropic layer (i.e., having up to 21 independent elastic moduli) is loaded over a finite portion of its top surface by a traction force

$$\mathbf{t}(z) e^{i\omega t} = [t_z(z)\hat{\mathbf{e}}_z + t_y(z)\hat{\mathbf{e}}_y] e^{i\omega t}, \tag{4}$$

where $\hat{\mathbf{e}}_i$ denotes a unit vector in the x_i coordinate direction. The tractions are assumed to be independent of the x-coordinate and therefore actually represent loading along a strip of infinite width in the x-direction.

We start the analysis from the purely acoustic form of the

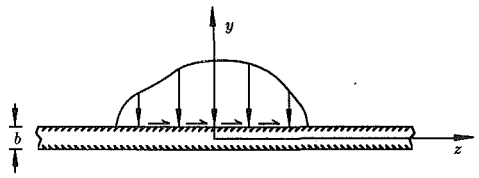

Fig. 1 Loading of an anisotropic layer by harmonic surface tractions

complex reciprocity relation (Auld, 1990b, pp. 154–155), relating any two solutions, 1 and 2, to the governing field equations (Eq. (1)). This relation can be written in differential form as

$$\nabla \cdot (\tilde{\mathbf{v}}_2 + \mathbf{T}_1 + \mathbf{v}_1 \cdot \tilde{\mathbf{T}}_2) = 0 \tag{5}$$

where $\mathbf{v}$ represents the particle velocity field and the tilde represents complex conjugation. In Eq. (5) both solutions, 1 and 2, are assumed to have the same frequency, ω, and the $e^{i\omega t}$ dependence of all field variables will be dropped for brevity.

The fields in the loaded waveguide are then expressed as a summation over all of the normal modes of the free layer, specified by index μ, multiplied by unknown, generally complex and z-dependent amplitudes, $A_\mu(z)$. For the field variables appearing in Eq. (5), these expansions are of the form

$$\mathbf{v}(y, z) = \sum_\mu A_\mu(z) \mathbf{v}_\mu(y) \tag{6a}$$

and

$$\mathbf{T}(y, z) = \sum_\mu A_\mu(z) \mathbf{T}_\mu(y). \tag{6b}$$

To determine the unknown mode amplitudes $A_\mu(z)$, in Eqs. (6*a–b*), the reciprocity relation, Eq. (5), is invoked with solution "1" being $\mathbf{v}$ and $\mathbf{T}$ appearing in Eqs. (6*a*) and (6*b*), and solution "2" being the νth mode of the free layer. That is

$$\mathbf{v}_2 = \mathbf{v}_\nu(y) e^{-i\beta_\nu z} \tag{7a}$$

$$\mathbf{T}_2 = \mathbf{T}_\nu(y) e^{-i\beta_\nu z}. \tag{7b}$$

Substituting Eqs. (6*a–b*) and (7*a–b*) into the reciprocity equation, Eq. (5), integrating the resulting equation across the waveguide thickness $-b/2 \le y \le b/2$ and making use of the fact that the normal modes satisfy traction-free boundary conditions results in a first-order ordinary differential equation which governs the amplitudes of the generated modes. For propagating modes, the wave number β_ν is real, and it can be shown by specializing a general equation in (Auld, 1990b, pg. 162) that, for the case considered here, the equation governing the amplitude of the generated modes reduces to the form

$$4P_{\nu\nu}\left(\frac{d}{dz} + i\beta_\nu\right) A_\nu(z) = \tilde{\mathbf{v}}_\nu(b/2) \cdot \mathbf{t}(z) \tag{8}$$

where the quantity $P_{\nu\nu}$ has been defined as

$$P_{\nu\nu} = \Re e\left(-\frac{1}{2}\int_{-b/2}^{b/2} \tilde{\mathbf{v}}_\nu \cdot \mathbf{T}_\nu \cdot \hat{\mathbf{e}}_z dy\right) \tag{9}$$

and $\Re e(\ )$ denotes real part of the quantity in brackets. From the definition of the acoustic Poynting vector (Auld, 1990a, pg. 155), this is recognized as the time-averaged power flow carried by the νth mode in the z-direction per unit waveguide width (in the x-direction) and has typical units of [Watts/m]. It should be remembered that, since the amplitudes of the modal fields themselves ($\mathbf{v}_\nu$ and $\mathbf{T}_\nu$) can be arbitrarily assigned (within the restrictions of infinitesimal elasticity theory), the power carried by the modes, Eq. (9), is also arbitrary, depending on the assigned amplitude. We will see that this indeterminacy will disappear in the final result, which will be independent of the arbitrary amplitude which may be assigned to $\mathbf{v}_\nu$ and $\mathbf{T}_\nu$.

Equation (8) is a first-order ordinary differential equation and can therefore be integrated using standard techniques. The solution can be written

$$A_\nu(z) = \frac{e^{-i\beta_\nu z}}{4P_{\nu\nu}} \int_c^z e^{i\beta_\nu \eta} \tilde{\mathbf{v}}_\nu(b/2) \cdot \mathbf{t}(\eta) d\eta, \tag{10}$$

where c is a constant used to satisfy the boundary condition on $A_\nu(z)$. Supposing that the external tractions, $\mathbf{t}$, are only nonzero in the interval $-L \le z \le L$, and using the boundary condition

$$A_\nu(z) = 0 \quad z \le -L \tag{11}$$

gives, for the amplitude of the rightward travelling modes,

$$A_\nu(z) = \frac{e^{-i\beta_\nu z}}{4P_{\nu\nu}} \int_{-L}^{L} e^{i\beta_\nu \eta} \tilde{\mathbf{v}}_\nu(b/2) \cdot \mathbf{t}(\eta) d\eta \quad z \ge L. \tag{12}$$

The corresponding expression for the leftward propagating modes can be obtained from Eq. (12) by replacing $P_{\nu\nu}$ by $-P_{\nu\nu}$, $\tilde{\mathbf{v}}_\nu$ by $\tilde{\mathbf{v}}_{-\nu}$, the wave number β_ν by $-\beta_\nu$ and finally by using the boundary condition $A_{-\nu} = 0$ for $z \ge L$. The result is

$$A_{-\nu}(z) = \frac{e^{i\beta_\nu z}}{4P_{\nu\nu}} \int_{-L}^{L} e^{-i\beta_\nu \eta} \tilde{\mathbf{v}}_{-\nu}(b/2) \cdot \mathbf{t}(\eta) d\eta \quad z \le -L. \tag{13}$$

Since the applied tractions vanish outside the interval $|z| > L$, the integration limits in Eqs. (12) and (13) can be extended indefinitely, i.e., to plus and minus infinity. The two equations can also be combined into

$$A_{\pm\nu}(z) = \frac{e^{\mp i\beta_\nu z}}{4P_{\nu\nu}} \tilde{\mathbf{v}}_{\pm\nu}(b/2) \cdot \int_{-\infty}^{\infty} e^{\pm i\beta_\nu \eta} \mathbf{t}(\eta) d\eta. \tag{14}$$

Having determined the expansion amplitudes, $A_{\pm\nu}(z)$, of the propagating modes (real β_ν), the fields in the loaded layer due to the propagating modes follow from the original expansions Eqs. (6*a*, *b*). For instance, the particle velocity field in the loaded layer can be written

$$\mathbf{v}(y, z) = \sum_\nu \left\{ \frac{e^{\mp i\beta_\nu z}}{4P_{\nu\nu}} \tilde{\mathbf{v}}_{\pm\nu}(b/2) \cdot \int_{-\infty}^{\infty} e^{\pm i\beta_\nu \eta} \mathbf{t}(\eta) d\eta \right\} \mathbf{v}_{\pm\nu}(y) + \sum_\nu A^e_{\pm\nu}(z) \mathbf{v}_{\pm\nu}(y). \tag{15}$$

For $z \ge L$, only the summation over the positive travelling (or decaying) modes (+) contribute whereas for $z \le -L$, only the summation over the negative travelling (or decaying) modes (−) contribute. The first summation represents the contribution of the propagating modes (real wave number, β_ν) and the second represents the contribution of the evanescent modes (imaginary and/or complex wave numbers) with expansion amplitudes $A^e_{\pm\nu}(z)$. Since the evanescent modes decay exponentially away from the source which excites them, the contribution from the second summation becomes smaller as z becomes larger. The actual distance from the source at which the amplitude of an evanescent mode becomes negligible depends on the magnitude of the imaginary part of its wave number.

Once the applied tractions, $\mathbf{t}(z)$, are specified, Eq. (14) can be used to determine the amplitudes of the forward and backward traveling modes which, when substituted into the original normal mode expansion, Eqs. (6*a*, *b*), gives that part of the total field in the loaded layer due to the propagating modes. The part of the total field due to the nonpropagating modes can also be determined by this procedure but their contribution is of less importance in nondestructive evaluation purposes since they decay exponentially from the source which excites them. Their amplitudes are not, however, given by Eq. (14), which is valid only for propagating modes. For the evanescent modes, the differential equation governing the amplitudes, Eq. (8), must be modified.

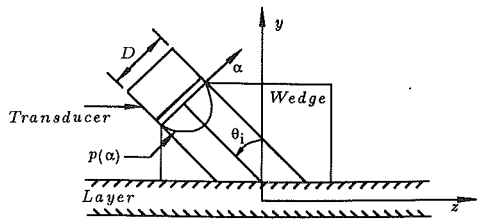

Fig. 2 Model of the "wedge method" of exciting guided waves. The transducer, of length, *D*, is mounted to a wedge and produces a plane wave with arbitrary pressure distribution, $p(\alpha)$, which impinges on the layer.

Specific Cases

It is now assumed that the tractions produced at the upper surface of the layer are due to loading by an ultrasonic transducer mounted to an angle beam "wedge" as shown in Fig. 2. The ultrasonic transducer is assumed to produce a time-harmonic plane stress wave which travels within the wedge and strikes the layer at a given angle θ_i. Beam spreading and beam shifting upon striking the layer are neglected, and the wedge is assumed to be coupled to the layer by a thin layer of nonviscous liquid. As a result, only normal tractions, $t_y(z)$, are assumed to be transferred, the shear tractions, $t_z(z)$, vanishing. Finally, the transducer is allowed to have an arbitrary pressure distribution, $p(\alpha)$, across its face. A similar problem, for isotropic layers and piston-like transducer, was solved using Fourier Integrals by Viktorov (1967).

Projecting $p(\alpha)$ on the the layer surface, the traction produced on the top of the layer is assumed to be of the form (neglecting an unnecessary phase factor and the $e^{i\omega t}$ dependence)

$$\mathbf{t}(z) = \begin{cases} p(z \cos\theta_i) |R(\theta_i)| e^{-ik_w \sin\theta_i z} \tilde{\mathbf{e}}_y, & \text{if } |z| \le L \\ 0, & \text{if } |z| > L \end{cases} \tag{16}$$

where $|R(\theta_i)|$ is a numerical factor introduced to account for the fact that the actual traction at the wedge-layer interface will in general be different than that due solely to the incident wave. It is assumed, however, that this factor is frequency independent and a discussion of this result, along with limited experimental verification, can be found in Ditri (1992). In Eq. (16), k_w represents the wave number of the incident wave in the wedge, numerically equal to ω/V_w, V_w representing the velocity of longitudinal waves in the wedge material.

Substituting this assumed form of surface traction into the general result, Eq. (14), gives, after some manipulation,

$$A_{\pm\nu}(z) = \frac{|R(\theta_i)|}{4} \frac{\tilde{v}_{\pm\nu y}(b/2)}{P_{\nu\nu}} \frac{e^{\mp i\beta_\nu z}}{\cos(\theta_i)} \int_{-\infty}^{\infty} p(\alpha) e^{\pm i\chi_\pm \alpha} d\alpha \tag{17}$$

where

$$\chi_+ \equiv \frac{\beta_\nu - k_w \sin\theta_i}{\cos\theta_i} \tag{18a}$$

$$\chi_- \equiv \frac{\beta_\nu + k_w \sin\theta_i}{\cos\theta_i} \tag{18b}$$

and $\tilde{v}_{\pm\nu y}$ represents the complex conjugate of the y-component of the particle velocity field of positive (+) and negative (−) propagating modes.

The appearance of the factor $P_{\nu\nu}$ in the denominator of Eq. (17) for the amplitudes ensures that the final result is independent of the arbitrarily chosen amplitude of $\mathbf{v}_\nu$. This is so because when A_ν of Eq. (17) is substituted into the normal mode expansions, Eqs. (6*a*, *b*), they contain products of the form $v_{\nu y}(b/2)\mathbf{v}_\nu(y)/P_{\nu\nu}$ and $v_{\nu y}(b/2)\mathbf{T}_\nu(y)/P_{\nu\nu}$. If $\mathbf{v}_\nu$ is replaced by $\alpha\mathbf{v}_\nu$ where α is an arbitrary complex constant, then owing to the linearity of the governing elasticity equations, $\mathbf{T}_\nu$

is also multiplied by the same factor. It follows that the terms $v_{\nu y}(b/2)\mathbf{v}_\nu(y)$ and $v_{\nu y}(b/2)\mathbf{T}_\nu(y)$ are multiplied by α^2. However, reference to Eq. (9) shows that $P_{\nu\nu}$ is also proportional to the product $\mathbf{v}_\nu(y)\cdot\mathbf{T}_\nu(y)$ and is therefore also multiplied by α^2. This ensures that the ratios $v_{\nu y}(b/2)\mathbf{v}_\nu(y)/P_{\nu\nu}$ and $v_{\nu y}(b/2)\mathbf{T}_\nu(y)/P_{\nu\nu}$ remain the same. Therefore, the final fields caused in the layer by the individual modes, Eqs. (6*a*, *b*), are independent of the arbitrarily assigned amplitudes of the modal fields which appear in their definitions. One could have started the normal mode expansion technique by expanding the fields in the loaded layer in terms of the power normalized normal modes, $\mathbf{v}_\nu/\sqrt{P_{\nu\nu}}$ and $\mathbf{T}_\nu/\sqrt{P_{\nu\nu}}$, which are already independent of the arbitrarily chosen multiplicative amplitudes for $\mathbf{v}_\nu$ and $\mathbf{T}_\nu$. In this case, $A_{\pm\nu}$ would have a $\sqrt{P_{\nu\nu}}$ factor instead of $P_{\nu\nu}$ in its denominator.

The integral appearing in Eq. (17) can be interpreted as the Fourier transform of the pressure distribution function $p(\alpha)$ with transform parameter χ given by Eqs. (18*a*) or (18*b*). It clearly exhibits the influence of the transducers pressure distribution on its guided wave generation characteristics.

In order to manifest clearly the physics of the excitation phenomenon, Eq. (17) is written in the form

$$A_{\pm\nu}(z) = \mathcal{G}\mathcal{F}^{(+)}E_{\pm\nu}e^{\mp i\beta_\nu z} \tag{19}$$

where

$$\mathcal{G} \equiv \frac{|R(\theta_i)|}{4} \tag{20a}$$

$$E_{\pm\nu} \equiv \frac{\tilde{v}_{\pm\nu y}(b/2)}{P_{\nu\nu}} \tag{20b}$$

$$\mathcal{F}^{(\pm)} \equiv \frac{1}{\cos(\theta_i)} \int_{-\infty}^{\infty} p(\alpha)e^{\pm i\chi\pm\alpha}d\alpha. \tag{20c}$$

The function $\mathcal{G}$ represents a numerical factor which depends solely on the output power of the transducer. The function $E_{\pm\nu}$, termed the "excitability" function of mode ν is seen to depend only on properties of the mode which is being excited and *not* on the properties of the source used for excitation. The function $\mathcal{F}^{(\pm)}$ is seen to depend only on properties of the transducer and wedge used to excite the layer. The product function, $\mathcal{F}\mathcal{G}$, which is also dependent only on transducer parameters, is termed the "excitation" function of the source. The amplitude with which guided waves are generated is therefore seen to be proportional to the product of the excitation function, $\mathcal{F}\mathcal{G}$, determined by transducer and wedge parameters, and the excitability function, $E_{\pm\nu}$, which depends on which mode is excited and where on its dispersion curve it is excited.

The actual pressure distribution of a transducer, $p(\alpha)$, depends essentially on how the transducer is manufactured. The simplest approximation to an actual pressure variation is the piston source defined by

$$p(\alpha) = \begin{cases} \sigma_o, & \text{if } |\alpha| \le \dfrac{D}{2} \\ 0, & \text{if } |\alpha| > \dfrac{D}{2} \end{cases}. \tag{21}$$

If this pressure variation is substituted into Eq. (17), the resulting expression for the excitation amplitudes is found to be

$$A_{\pm\nu}(z) = \frac{\sigma_o|R(\theta_i)|}{4}\frac{\tilde{v}_{\pm\nu y}(b/2)}{P_{\nu\nu}} 2\frac{\sin\left(\dfrac{(\beta_\nu \mp k_w \sin\theta_i)D}{2\cos\theta_i}\right)}{(\beta_\nu \mp k_w \sin\theta_i)} e^{\mp i\beta_\nu z} \tag{22}$$

where the positive amplitudes are valid for $z \ge L$ and the negative amplitudes for $z \le -L$. Comparing Eq. (22) with Eq. (19) shows that for a piston source transducer, $\mathcal{G} = \sigma_o|R(\theta_i)|/4$, $E_{\pm\nu} = \tilde{v}_{\pm\nu y}(b/2)/P_{\nu\nu}$ and

$$\mathcal{F}^{(\pm)}_{\text{Piston}} = 2\frac{\sin\left(\dfrac{(\beta_\nu \mp k_w \sin\theta_i)D}{2\cos\theta_i}\right)}{(\beta_\nu \mp k_w \sin\theta_i)}, \tag{23}$$

which is, except for notation, identical to the result found by (Viktorov, 1967, pp. 83–93) when treating the problem of the excitation of isotropic layers using piston sources by Fourier integral techniques. It is interesting to note from Eq. (22) that, unlike the case of infinite plane wave excitation, Snell's law is not rigorously applicable in describing the generation process of Lamb waves when using finite sources since the amplitude function is nonzero for a range of wave numbers (or phase velocities) instead of being nonzero for just the single wave number determined by Snell's law (Eq. (25)). The most common method found in the literature of determining the appropriate shoe angle to use when trying to generate a Lamb wave mode of phase velocity V_{ph} is the use of Snell's law,

$$\theta_i = \sin^{-1}\left(\frac{V_w}{V_{\text{ph}}}\right), \tag{24}$$

where V_w is the longitudinal wave velocity in the shoe material (or coupling fluid if immersion is used). In terms of wave numbers, this relation can be written

$$\beta = k_w \sin\theta_i, \tag{25}$$

that is, it is usually assumed that, given an incident angle, θ_i, and incident wave number, k_w, only a single wave number, given by Snell's law, can be generated, or will at least be the dominant wave number of the generated waves.

Although the function $\mathcal{F}^{(+)}_{\text{Piston}}$ is strictly not defined when Eq. (25) is satisfied, it can be defined as the limit,

$$\mathcal{F}^{(+)}_{\text{Piston}}|_{\beta=k_w\sin\theta_i} \equiv \lim_{\beta\to k_w\sin\theta_i} \mathcal{F}^{(+)}_{\text{Piston}} = \frac{D}{\cos\theta_i}, \tag{26}$$

in which case $\mathcal{F}^{(+)}_{\text{Piston}}$ will be continuous for all β and have a maximum at the Snell's law wave number $\beta = k_s \sin(\theta_i)$. Equation (22) then shows that for $\beta_\nu \ne k_w \sin\theta_i$, $\mathcal{F}^{(-)}_{\text{Piston}}$ and $\mathcal{F}^{(+)}_{\text{Piston}}$ do not vanish identically, even though they decrease as β_ν becomes different than $k_w \sin(\theta_i)$. Therefore, even if the Snell's Law angle is not used, the mode can still be generated, albeit less efficiently.

We can define a "wave number bandwidth," σ_β, associated with the piston transducer as the value of $\beta - k_s \sin\theta_i$ where the function $\mathcal{F}^{(+)}_{\text{Piston}}$ decreases to say $1/e$ (≈ -9dB) its maximum, that is, $\mathcal{F}^{(+)}_{\text{Piston}}(\beta - k_s\sin\theta_i = \pm\sigma_\beta) = \mathcal{F}^{(+)}_{\text{Piston}}(0)/e$. This value is given, approximately, by

$$\sigma_\beta \approx \frac{4.398\cos\theta_i}{D}. \tag{27}$$

As can be seen from Eq. (27), as $D \to \infty$, $\sigma_\beta \to 0$, i.e., for plane wave incidence (infinite diameter transducer) the wave number bandwidth is zero, so only one value of wave number can be excited as given by Snell's Law, Eq. (25). For a finite-sized piston source transducer, we see that the wave number bandwidth is inversely proportional to the diameter D. The bandwidth is directly proportional to $\cos\theta_i$ which in the interval $0 \le \theta_i < 90$ deg decreases monotonically from 1.0 to 0.0. Recognizing $D/\cos\theta_i$ as the length of the loaded region (see Fig. 2), we can conclude that the wave number bandwidth *decreases* as the size of the insonification region *increases*.

Figure 3 is a parametric plot of $\mathcal{F}^{(+)}_{\text{Piston}}$ with the size of the loading region, $D/\cos\theta_i$ as the parameter (in all plots, $\omega = 2$ [rad/μsec]). As can be seen, as the insonification region becomes larger, the transducer-wedge source becomes more and more selective to the Snell's Law wave number $k_w \sin(\theta_i)$.

A somewhat more realistic model of an actual ultrasonic

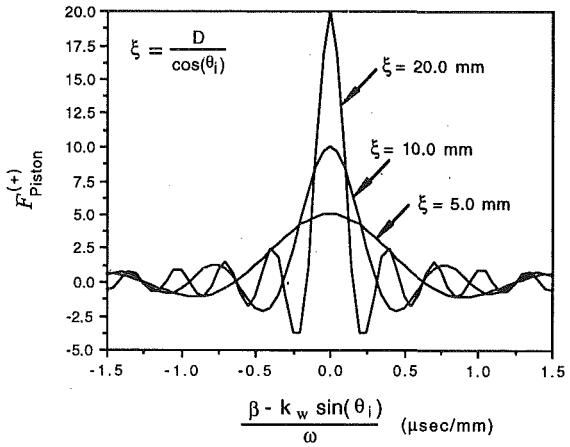

Fig. 3 Parametric plots of the $\mathcal{F}^{(+)}_{Piston}$ with the size of the loading region as the parameter (ω = 2 rad/μsec)

transducer is a parabolic pressure distribution. In this case, the pressure distribution function $p(\alpha)$ can be written

$$p(\alpha) = \begin{cases} \sigma_o\left(1 - \dfrac{\alpha^2}{(D/2)^2}\right), & \text{if } |\alpha| \le \dfrac{D}{2} \\ 0, & \text{if } |\alpha| > \dfrac{D}{2} \end{cases} \tag{28}$$

where σ_o now represents the maximum pressure which occurs at the center of the transducer face, $\alpha = 0$.

Substituting Eq. (28) into Eq. (17) and comparing the result with Eq. (19) shows that

$$\mathcal{F}^{(+)}_{Parabolic}(\chi_+) = \frac{8}{D\cos(\theta_i)\chi_+^2}\left[\frac{2\sin\left(\chi_+ \dfrac{D}{2}\right)}{D\chi_+} - \cos\left(\chi_+ \frac{D}{2}\right)\right], \tag{29}$$

where χ_+ is defined in Eq. (18*a*).

Again, we can define the wave number bandwidth of the parabolic source transducer, σ_β, to be the value of $\beta - k_s \sin\theta_i$ at which $\mathcal{F}^{(+)}_{Parabolic}$ drops to $1/e$ its maximum value (at $\chi_+ = 0$). Performing the calculations results in, approximately,

$$\sigma_\beta \approx \frac{5.852\cos\theta_i}{D}. \tag{30}$$

Comparing this bandwidth with that obtained for the Piston source, Eq. (27), shows that the parabolic source has a somewhat *wider* wave number bandwidth. The dependence of σ_β on the transducer diameter, D, and the incident angle, θ_i, is the same as for the piston transducer.

It is important to know how the transducer parameters (or equivalently the wave number bandwidth) influences the range of *phase velocities* which may be generated by the applied source. Due to the finite size of the loading region, there is actually a range of phase velocities within which the magnitude of $\mathcal{F}^{(+)}$ (for both piston and parabolic sources) remains above, say -9dB of its maximum value. As a result, it should be expected that any mode who's dispersion curve passes through this phase velocity region (for the given frequency ω) may be excited by the source while modes whose dispersion curves are far from this region should contribute less to the total generated field. How strongly each mode is generated also depends on the value of its excitability function E_ν at this frequency.

To get an estimate of the range of phase velocities within which significant excitation may occur, we can use the definition of the wave number bandwidth σ_β. Recalling that σ_β is

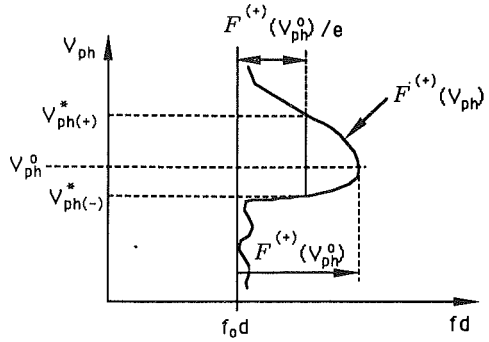

Fig. 4 Definitions of the lower, $V^*_{ph(-)}$, and upper, $V^*_{ph(+)}$, phase velocities where $\mathcal{F}^{(+)}$ drops by approximately 9 dB

the value of $\beta - k_s \sin\theta_i$ where the function $\mathcal{F}^{(+)}$ drops to $1/e$ ($\approx -9dB$) its maximum value (at $\beta = k_w \sin\theta_i$), we have

$$\mathcal{F}^{(+)}(\beta - k_s \sin\theta_i) = \mathcal{F}^{(+)}(0)/e \Rightarrow \beta - k_w \sin\theta_i = \pm\sigma_\beta$$

$$\Rightarrow \omega\left(\frac{1}{V^*_{ph}} - \frac{1}{V^o_{ph}}\right) = \pm\sigma_\beta \tag{31}$$

where V^*_{ph} is the phase velocity at which $\mathcal{F}^{(+)}$ drops by 9 *dB* of its maximum value and $V^o_{ph} = V_w/\sin\theta_i$. Considering the plus and minus signs in the above equality we can solve for two values of V^*_{ph} which we denote by $V^*_{ph(-)}$ and $V^*_{ph(+)}$. These are given by

$$V^*_{ph(-)} = \frac{\omega V^o_{ph}}{\omega + \sigma_\beta V^o_{ph}} \tag{32}$$

and

$$V^*_{ph(+)} = \frac{\omega V^o_{ph}}{\omega - \sigma_\beta V^o_{ph}}. \tag{33}$$

These velocities, under certain conditions to be developed shortly, represent the values of phase velocity at which the function $\mathcal{F}^{(+)}$ (considered as a function of phase velocity) drops by 9 dB of its maximum value which occurs at $V_{ph} = V^o_{ph}$. $V^*_{ph(-)}$ represents the velocity *smaller than* V^o_{ph} at which $\mathcal{F}^{(+)}$ drops by 9 dB and $V^*_{ph(+)}$ represents the velocity *larger than* V^o_{ph} at which $\mathcal{F}^{(+)}$ drops by 9 dB (Fig. 4).

Having $V^*_{ph(-)}$ and $V^*_{ph(+)}$, we can calculate the range of phase velocities over which significant excitation may occur, $V^*_{ph(+)} - V^*_{ph(-)}$. As a percent of the Snell's Law velocity, V^o_{ph} (at which $\mathcal{F}^{(+)}$ is maximum), this range is given by

$$\sigma_v \equiv \frac{V^*_{ph(+)} - V^*_{ph(-)}}{V^o_{ph}} = \frac{2\sigma_\beta\left(\dfrac{V^o_{ph}}{\omega}\right)}{1 - \sigma_\beta^2\left(\dfrac{V^o_{ph}}{\omega}\right)^2}. \tag{34}$$

The quantity σ_v will hereafter be called the "-9 dB Phase Velocity Bandwidth" or (-9 dB PVB) of the transducer-wedge combination. Equation (34) for the -9 dB PVB is only valid in the range $0 \le \sigma_\beta \le \omega/V^o_{ph}$. This is due to the fact that, while $V^*_{ph(-)}$ remains valid for $0 \le \sigma_\beta < \infty$ (i.e., for any value of σ_β it represents the value of phase velocity, smaller than V^o_{ph}, at which $\mathcal{F}^{(+)}$ drops by 9 dB), $V^*_{ph(+)}$ is only defined for $0 \le \sigma_\beta < \omega/V^o_{ph}$. As σ_β approaches ω/V^o_{ph}, the upper velocity at which $\mathcal{F}^{(+)}$ drops by 9 dB (i.e., $V^*_{ph(+)}$) quickly approaches infinity. For $\sigma_\beta > \omega/V^o_{ph}$, $V^*_{ph(+)}$ becomes negative and there is no longer an upper value of phase velocity at which $\mathcal{F}^{(+)}$ will drop by 9 dB. Instead, it asymptotically approaches some finite value *above* the -9 dB values as $V_{ph} \to \infty$. Therefore, the -9 dB phase velocity bandwidth approaches infinity as $\sigma_\beta \to \omega/V^o_{ph}$ and we will say that it is infinite for $\sigma_\beta > \omega/V^o_{ph}$

with the understanding that this means that there is no upper velocity at which $\mathfrak{F}^{(+)}$ drops by 9 dB of its maximum value.

Making use of the relation $V^o_{\text{ph}}/\omega = \lambda^o/2\pi$ and the fact that the wave number bandwidths of both the piston and parabolic sources can be written as $\sigma_\beta = K\cos(\theta_i)/D$ (see Eqs. (27) and (30)), the -9 dB phase velocity bandwidth can be written

$$\sigma_v = \frac{\dfrac{K}{\pi}\left(\dfrac{\lambda^o}{D}\right)}{1-\left(\dfrac{K}{2\pi}\right)^2\left(\dfrac{\lambda^o}{D}\right)^2}, \tag{35}$$

where $\overline{D} \equiv D/\cos(\theta_i)$ represents the length of the insonification region, $\lambda^o \equiv 2\pi V^o_{\text{ph}}/\omega$, and $K = 4.398$ for piston sources or 5.852 for parabolic sources.

Equation (35) shows that, for a given source, the -9 dB PVB depends *only* on the ratio of the length of the insonification region to the wavelength at the chosen phase velocity and frequency and that the -9 dB PVB approaches zero as this ratio approaches infinity.

Physically, this is a manifestation of the fact that if the wavelength is very small compared to the size of the insonification region, the waveguide modes generated in the layer can properly "phase match" to the incident wave field and hence, due to destructive interference, will have a narrow phase velocity spectrum. On the other hand, for large wavelengths compared to the size of the insonification region, the generated wave modes cannot properly phase match to the incident field and the generated modes may be excited over a significant range of phase velocities. Because the guided wave modes are more or less excitable at different points of their dispersion curves (determined by their excitability functions), this means that the modes may actually be generated more strongly at phase velocities other than that given by Snell's Law even though the excitation function $\mathfrak{F}^{(+)}$ is maximum at the Snell's Law phase velocity.

Transient Loading

The results presented thus far were for harmonic excitation at a single but arbitrary frequency ω. The excitation amplitudes, $A_{\pm\nu}$, are therefore frequency dependent. If the transducer mounted to the wedge actually has a frequency spectrum, say $\hat{g}(\omega)$, then, by linear superposition, the total fields in the loaded waveguide can be expressed as integrals over frequency (times thickness product) $\Omega \equiv fd$. For instance, the velocity field in front of $(+)$ or behind $(-)$ the transducer due to the propagating modes, $\mathbf{v}_p$, can be written (Ewing et al., 1957) as

$$\mathbf{v}_p^{(\pm)}(y, z, t) = \int \left(\sum_\mu A_{\pm\mu}(z, \Omega, V_{\text{ph}})\mathbf{v}_{\pm\mu}(y, \Omega, V_{\text{ph}})e^{i\frac{2\pi\Omega}{d}t}\right)d\Omega \tag{36}$$

where now $\mathcal{G}$ which appears in the definition of $A_{\pm\nu}$ is given by $\mathcal{G} = \hat{g}(\Omega)|R(\theta_i)|/4$ and since we are considering only propagating modes, the limits of the integration extend from the cutoff fd of the given mode to infinity. Also, the index μ is taken to include only the propagating modes of the structure at a given frequency thickness product Ω.

Since there are only a finite number of propagating modes at any frequency thickness product, the summation in Eq. (36) contains a finite number of terms. We can therefore interchange the summation and integration, in which case, Eq. (36) can be written

$$\mathbf{v}_p^{(\pm)}(y, z, t) = \sum_\mu \int A_{\pm\mu}(z, \Omega, V_{\text{ph}})\mathbf{v}_{\pm\mu}(y, \Omega, V_{\text{ph}})e^{i\frac{2\pi\Omega}{d}t}d\Omega$$

$$= \sum_\mu \int \mathcal{G}(\Omega)E_{\pm\mu}\mathfrak{F}^{(\pm)}(V_{\text{ph}}, \Omega)\mathbf{v}_{\pm\mu}(y, \Omega, V_{\text{ph}})e^{i\left(\frac{2\pi\Omega}{d}t\mp\beta_\mu z\right)}d\Omega. \tag{37}$$

Since the phase velocity V_{ph} and frequency thickness Ω of a given mode μ are restricted to lie on that modes' dispersion curve, each of the integrals in Eq. (37) are actually along the dispersion curves of the individual modes. It is interesting to note that even when integral transform techniques are used to solve waveguide loading problems, a similar form (i.e., summation of dispersion curve integrals) results for the excited fields (Achenbach, 1973; Miklowitz, 1978). However, the present technique gives a direct physical interpretation to the integrand whereas the integral transform technique does not. Some limited experimental verification of Eq. (37), comparing

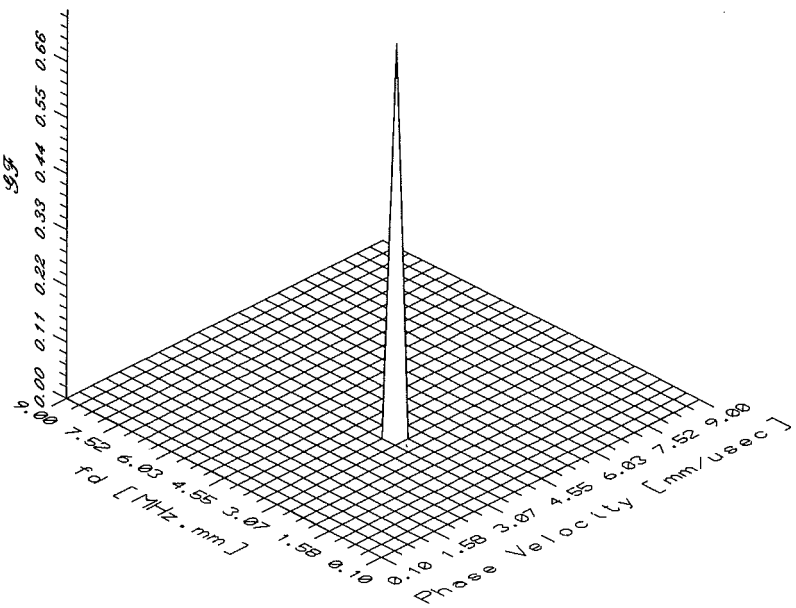

Fig. 5 Plot of the magnitude of the excitation function, $|\mathcal{G}\mathfrak{F}^{(+)}_{\text{Piston}}|$ for a transducer of length $1 \cdot 10^5$ mm (3,937 in.), central frequency of 3.5 MHz, -9 dB frequency bandwidth of .5 MHz, mounted to a wedge of angle 45 deg with longitudinal velocity 2.7 mm/μsec

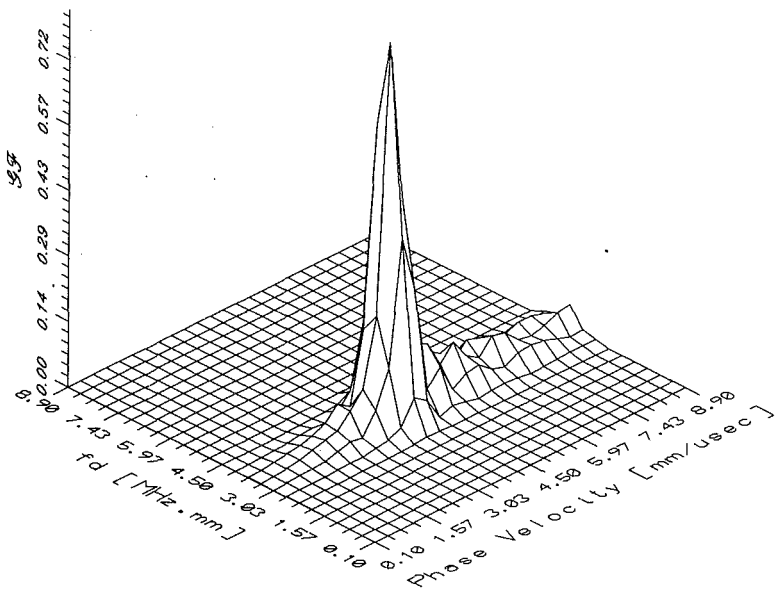

Fig. 6 Same as Fig. 5, except for a transducer length of 6.35 mm (1/4 in.)

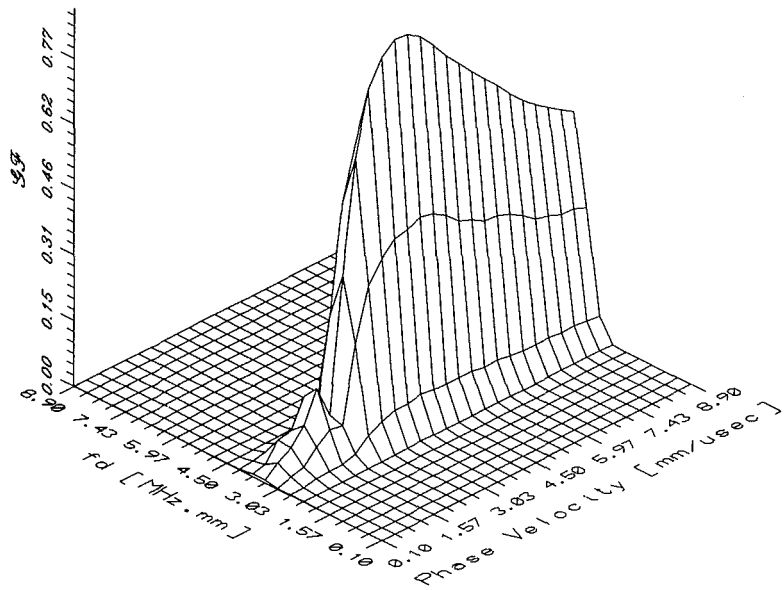

Fig. 7 Same as Fig. 5, except for a transducer length of 0.77 mm (1/33 in.)

experimentally obtained RF signals with the numerical evaluation of Eq. (37) for specific y and z can be found in Ditri, (1992).

The two functions $\mathcal{G}(\Omega)$ and $\mathcal{F}(V_{\text{ph}}, \Omega)$ determine the region in the phase velocity-frequency thickness plane in which the transducer-wedge combination is most capable of exciting waveguide modes.

Figures 5 through 7 illustrate the effect of the transducer diameter, D, on the excitation function $\mathcal{G}(\Omega)\mathcal{F}(V_{\text{ph}}, \Omega)$, and hence, on the selectivity of the transducer-wedge combination to a particular phase velocity and frequency. The transducer is assumed to have a Gaussian frequency spectrum

$$\hat{g}(\Omega) = Ae^{-\left(\frac{\Omega-\Omega_o}{\sigma_t}\right)^2}, \tag{38}$$

where the central frequency is taken as 3.5 MHz and the frequency bandwidth, σ_t, is taken as 0.5 MHz (for a 1 mm thick layer). The transducer is also assumed to generate a piston pressure profile and therefore $\mathcal{F}^{(+)}$ represents $\mathcal{F}^{(+)}_{\text{Piston}}$ given by Eq. (23). The figures are surface plots of the magnitude of the excitation function, $|\mathcal{G}(\Omega)\mathcal{F}(V_{\text{ph}}, \Omega)|$, over the phase velocity $-fd$ plane. The figures show the effect of varying the diameter of the transducer for fixed incident angle, frequency, and frequency bandwidth, and hence, varying the ratio $\overline{D}/\lambda^o$. The constant parameters in all the plots are a center frequency of 3.5 MHz, a frequency bandwidth (σ_t) of 0.5 MHz, an incident angle of 45 deg, and a shoe with longitudinal velocity, V_w, of 2.7 mm/μsec (Plexiglass). This gives a wavelength, λ^o, at the peak frequency, 3.5 MHz, of 1.09 mm. The parameter which is varied is the diameter of the transducer (D) and hence the size of the loading region on the layer, $\overline{D} = D/\cos\theta_i$. Since the wavelength, λ^o, remains the same for each plot, decreasing $\overline{D}$ decreases the ratio $\overline{D}/\lambda^o$. The diameters used in Figs. 5–7, as well as the calculated wave number and phase velocity bandwidths are given in Table 1.

In each of the plots, one should imagine the dispersion curves

of the particular layer under consideration as being superimposed on the underlying grid of phase velocity versus fd. Then, the amplitude with which each mode, μ, is generated at each particular point of its dispersion curve is given by the product of the excitability of the mode at that point, $E_\mu(\Omega, V_{ph})$, with the amplitude of the $\mathcal{GF}$ surface at that point. Therefore, the sharper the peak of the $\mathcal{GF}$ surface, the more selective the transducer-shoe combination is to a particular mode at a particular point on its dispersion curve.

As can be seen from Figs. 5-7 and Table 1, the selectivity of the transducer-wedge combination to a particular phase velocity becomes worse and worse as the ratio of the insonification region to the wavelength at the central frequency, $\overline{D}/\lambda^o$ is decreased. Figure 5 is used to illustrate the fact that if a plane wave is incident (extremely large D), then there is essentially only one value of phase velocity which can be generated with any appreciable intensity and it is given by Snell's Law once the material properties of the wedge and the incident angle are known. Figure 6 illustrates that when $\overline{D}/\lambda^o \sim 10$ the selectivity of the transducer-wedge combination is still highly peaked at the Snell's Law phase velocity but that the width of the peak (in the phase velocity direction) at the -9 dB point is now around 17 percent of the Snell's Law velocity. Finally, Fig. 7 shows that when $\overline{D}/\lambda^o \sim 1$, the transducer-wedge combination has virtually no selectivity to phase velocity since the excitation function remains over -9 dB of its maximum over a 275 percent velocity range.

An illustration of the fact that it is the ratio $\overline{D}/\lambda^o$ and not merely the size of the transducer, which determines the selectivity of the transducer to a particular phase velocity, Fig. 8 and 9, are parametric plots where the diameter and all frequency parameters are kept the same as in the previous figures while the incident angle is varied. This has the effect of varying the Snell's Law phase velocity, V^o_{ph}, and hence the wavelength $\lambda^o \equiv 2\pi V^o_{ph}/\omega$. For a given diameter transducer, the insonified region, $\overline{D}$, increases as the incident angle does. The net result is that although the transducer diameter, D, is kept constant in all plots, the ratio of loading length to wavelength, $\overline{D}/\lambda^o$ is being varied. The incident angles used in Figs. 8-9 are given in Table 2 along with the calculated Snell's Law phase velocities, and wave number and phase velocity bandwidths.

It can be seen from Figs. 8-9 that a given diameter transducer, with a given central frequency and frequency bandwidth, can be more or less selective in phase velocity depending on the incident angle θ_i. This is actually a manifestation of the fact that the ratio of loading region to wavelength $\overline{D}/\lambda^o$ increases with increasing incident angle.

Conclusions

The problem of the excitation of generally anisotropic layers by applied surface tractions has been analyzed using the normal mode expansion technique. Two loading configurations, typical of those used in nondestructive evaluation for generating waveguide modes, have been examined in detail. It has been shown how the relevant parameter in determining the selectivity of the source to a specific phase velocity is the ratio of the length of the loaded region, $\overline{D}$, to the wavelength in the phase velocity-frequency thickness plane, λ^o. It was demonstrated that for $\overline{D}/\lambda^o$ greater than approximately 10, the significant excitation (above -9 dB of the maximum) may occur over an approximately 17 percent range, whereas for $\overline{D}/\lambda^o \sim 1$ there is virtually no selectivity to a particular phase velocity.

Acknowledgments

Thanks are given to the Federal Aviation Agency in Atlantic City, NJ, and to the NASA Lewis Research Center, Cleveland, OH, for partial support of this work. Special thanks are given to Dave Galella of the FAA and Alex Vary of NASA.

Table 1 Parameters used in Figs. 5 through 7

Figure	D (mm) (in.)	$\overline{D}/\lambda^o$	σ_β (1/mm)	σ_v • 100 percent
5	$1.0 \cdot 10^5$ (3937)	$3.29 \cdot 10^6$	$1.22 \cdot 10^{-6}$	$4.233 \cdot 10^{-5}$
6	6.35 (1/4)	8.24	0.490	17.13
7	0.77 (1/33)	1.00	4.035	274.57

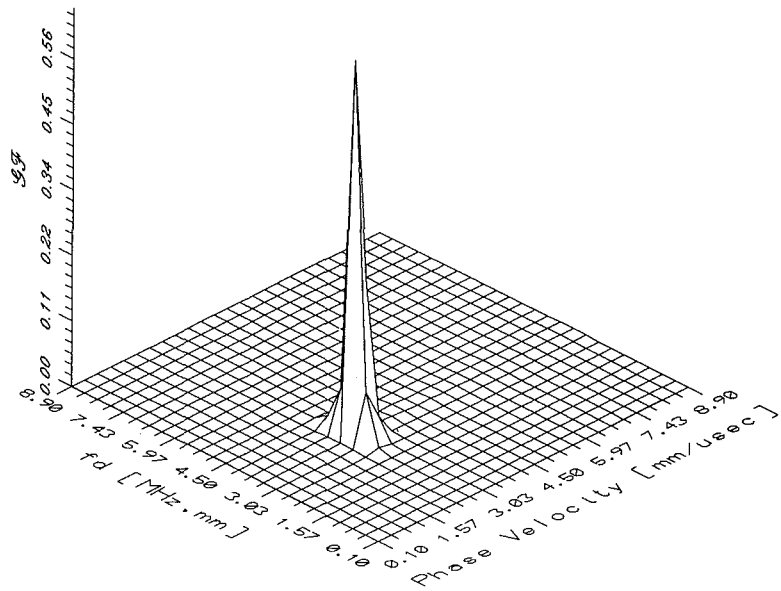

Fig. 8 Plot of the magnitude of the excitation function, $|\mathcal{GF}^{(+)}_{Piston}|$ for a transducer of length 25.4 mm (1 in.), central frequency of 3.5 MHz, -9 dB frequency bandwidth of .5 MHz, mounted to a wedge of angle 80 deg with longitudinal velocity 2.7 mm/μsec

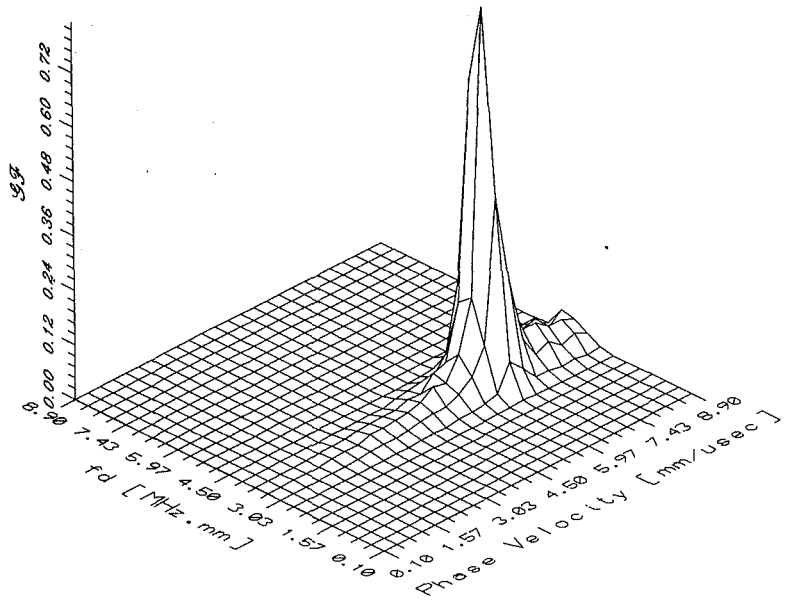

Fig. 9 Same as Fig. 8, except for an incident angle of 25 deg

Table 2 Parameters used in Figs. 8 and 9

Figure	D (mm)	θ_i (Deg)	V_{ph}^o	$\overline{D}/\lambda^o$	σ_β (1/mm)	σ_v • 100 percent
8	25.40	80	2.74	186.73	0.024	0.59
9	25.40	25	6.38	15.35	0.286	16.76

References

Achenbach, J. D., 1973, *Wave Propagation in Elastic Solids*, Elsevier, New York, NY, pp. 331-342.

Auld, B. A., and Kino, G. S., 1971, "Normal Mode Theory for Acoustic Waves and Their Application to the Interdigital Transducer," *IEEE Trans.* Vol. ED-18, pp. 898-908.

Auld, B. A., 1990a, *Acoustic Fields and Waves in Solids*, Vol. I, 2nd ed., Kreiger, FL.

Auld, B. A., 1990b, *Acoustic Fields and Waves in Solids*, Vol. II, 2nd ed., Kreiger, FL.

Bendec, F., Peretz, M., and Rokhlin, S. I., 1984, "Ultrasonic Lamb Wave Method for Sizing of Spot Welds," *Ultrasonics*, Vol. 22, No. 2, pp. 78-84.

Datta, S. K., Shah, A. H., Chakraborty, T., and Bratton, R. L., 1988, "Wave Propagation in Laminated Composite Plates: Anisotropy and Interface Effects," *Wave Propagation in Structural Composites*, AMD-Vol. 90, A. K. Mal, and T. C. T. Ting, eds., ASME, New York, pp. 39-52.

Ditri, J. J., and Rose, J. L., 1992, "Excitation of Guided Elastic Wave Modes in Hollow Cylinders by Applied Surface Tractions," *J. Appl. Phys.*, Vol. 72, No. 7, pp. 2589-2597.

Ditri, J. J., 1992, "Some Theoretical and Experimental Aspects of the Generation of Guided Elastic Waves Using Finite Sources," Ph.D. Thesis, Drexel University, Philadelphia, PA.

Ewing, W. M., Jardetsky, W. S., and Press, F., 1956, *Elastic Waves in Layered Media*, McGraw-Hill, New York, pp. 61-62.

Folk, R., Herczynski, A., 1986, "Solutions of Elastodynamic Slab Problems Using a New Orthogonality Condition," *J. Acoust. Soc. Am.*, Vol. 80, No. 4, pp. 1103-1110.

Herczynski, A., and Folk, R., 1989, "Orthogonality Conditions for the Pochammer—Chree Modes," *Q. Jl. Mech. Appl. Math.*, Vol. 42, Pt. 4, pp. 523-536.

Karim, M. R., Mal, A. K., and Bar-Cohen, Y., 1990, "Determination of the Elastic Constants of Composites Through Inversion of Leaky Lamb Wave Data," *Review of Progress in Quantitative NDE*, D. O. Thompson and D. E. Chimenti, eds., Vol. 9.

Kino, G. S., 1987, *Acoustic Waves: Devices, Imaging and Digital Signal Processing*, Prentice-Hall, Englewood Cliffs, NJ.

Li, Y., Thompson, R. B., 1990, "Influence of Anisotropy on the Dispersion Characteristics of Guided Ultrasonic Plate Modes," *J. Acoust. Soc. Am.*, Vol. 87, No. 5, pp. 1911-1931.

Mal, A. K., Gorman, M., and Prosser, W., 1992, "Material Characterization of Composite Laminates Using Low Frequency Plate Wave Dispersion Data," *Review of Progress in Quantitative NDE*, D. O. Thompson and D. E. Chimenti, eds. , Vol. 11B, pp. 1451-1458.

Miklowitz, J., 1978, *The Theory of Elastic Waves and Waveguides*, North-Holland, New York, pp. 409-430.

Nayfeh, A. H., Taylor, T. W., and Chimenti, D. E., 1988, "Theoretical Wave Propagation in Multilayered Orthotropic Media," ASME, *Wave Propagation in Structural Composites*, AMD-Vol. 90, A. K. Mal, and T. C. T. Ting, eds., ASME, New York, pp. 17-27.

Pilarski, A., and Rose, J. L., 1992, "Utility of Subsurface Longitudinal Waves in Composite Material Characterization," *Journal of Nondestructive Evaluation*, to be published.

Rokhlin, S. I., Wu, C. Y., and Wang, L., 1990, "Application of Coupled Ultrasonic Plate Modes for Elastic Constant Reconstruction of Anisotropic Materials," *Review of Progress in Quantitative NDE*, D. O. Thompson and D. E. Chimenti, eds., Vol. 9, pp. 1403-1410.

Solie, L. P., and Auld, B. A., 1972, "Elastic Waves in Free Anisotropic Plates," *J. Acoust. Soc. Am.*, Vol. 54, No. 1, pp. 50-65.

Spetzler, H., and Datta, S., 1990, "Experimental Flaw Detection by Scattering of Plate Waves," *Elastic Waves and Ultrasonic Nondestructive Evaluation*, S. K. Datta, J. D. Achenbach, and Y. S. Rajapakse eds., Elsevier, New York, pp. 135-141.

Viktorov, I. A., 1967, *Rayleigh and Lamb Waves, Physical Theory and Applications*, Plenum Press, New York.